



# HHS Public Access

## Author manuscript

*Neurochem Res.* Author manuscript; available in PMC 2018 February 20.

Author Manuscript

Author Manuscript

Author Manuscript

Author Manuscript

Published in final edited form as:

*Neurochem Res.* 2016 November ; 41(11): 2836–2847. doi:10.1007/s11064-016-1998-6.

## Effects of a Standardized Phenolic-Enriched Maple Syrup Extract on $\beta$ -Amyloid Aggregation, Neuroinflammation in Microglial and Neuronal Cells, and $\beta$ -Amyloid Induced Neurotoxicity in *Caenorhabditis elegans*

Hang Ma<sup>1</sup>, Nicholas A. DaSilva<sup>1</sup>, Weixi Liu<sup>1</sup>, Pragati P. Nahar<sup>1</sup>, Zhengxi Wei<sup>1</sup>, Yongqiang Liu<sup>1</sup>, Priscilla T. Pham<sup>2</sup>, Rebecca Crews<sup>2</sup>, Dhiraj A. Vattem<sup>2</sup>, Angela L. Slitt<sup>1</sup>, Zahir A. Shaikh<sup>1</sup>, and Navindra P. Seeram<sup>1,\*</sup>

<sup>1</sup>Department of Biomedical and Pharmaceutical Sciences, College of Pharmacy, University of Rhode Island, Kingston, RI 02881, United States

<sup>2</sup>Nutrition Biomedicine and Biotechnology, Texas State University, San Marcos, TX 78666, United States

### Abstract

Published data supports the neuroprotective effects of several phenolic-containing natural products, including certain fruit, berries, spices, nuts, green tea, and olive oil. However, limited data are available for phenolic-containing plant-derived natural sweeteners including maple syrup. Herein, we investigated the neuroprotective effects of a chemically standardized phenolic-enriched maple syrup extract (MSX) using a combination of biophysical, *in vitro*, and *in vivo* studies. Based on biophysical data (Thioflavin T assay, transmission electron microscopy, circular dichroism, dynamic light scattering, and zeta potential), MSX reduced amyloid  $\beta_{1-42}$  peptide ( $A\beta_{1-42}$ ) fibrillation in a concentration-dependent manner (50–500  $\mu$ g/mL) with similar effects as the neuroprotective polyphenol, resveratrol, at its highest test concentration (63.5% at 500  $\mu$ g/mL vs. 77.3% at 50  $\mu$ g/mL, respectively). MSX (100  $\mu$ g/mL) decreased  $H_2O_2$ -induced oxidative stress (16.1% decrease in ROS levels compared to control), and down-regulated the production of lipopolysaccharide (LPS)-stimulated inflammatory markers (22.1, 19.9, 74.8, and 87.6% decrease in NOS, IL-6, PGE<sub>2</sub>, and TNF $\alpha$  levels, respectively, compared to control) in murine BV-2 microglial cells. Moreover, in a non-contact co-culture cell model, differentiated human SH-SY5Y neuronal cells were exposed to conditioned media from BV-2 cells treated with MSX (100  $\mu$ g/mL) and LPS or LPS alone. MSX-BV-2 media increased SH-SY5Y cell viability by 13.8% compared to media collected from LPS-BV-2 treated cells. Also, MSX (10  $\mu$ g/mL) showed protective effects against  $A\beta_{1-42}$  induced neurotoxicity and paralysis in *Caenorhabditis elegans* *in vivo*. These data support the potential neuroprotective effects of MSX warranting further studies on this natural product.

\* Author to whom correspondence should be addressed: N.P.S.: Phone/Fax: 401-874-9367/5787; nseeram@uri.edu.

### Conflict of interest statement

The authors have declared no conflicts of interest.

### Supplementary Materials

Supplementary data associated with this article can be found in the online version.

## Keywords

Maple syrup phenolics; neuroprotective; neuroinflammation; amyloid  $\beta_{1-42}$ ; *Caenorhabditis elegans*; Alzheimer's disease

## Introduction

Microglia cells are resident immune cells in the central nervous system which can be activated by abnormalities including oxidative and inflammatory stresses [1]. Chronic activation of microglia cells leads to the production of pro-inflammatory cytokines including nitric oxide synthase (NOS), interleukins, prostaglandins (PGs), and tumor necrosis factor  $\alpha$  (TNF $\alpha$ ) [2]. These neurotoxic inflammatory factors result in massive neuronal cell death and are linked to several neurodegenerative diseases including Alzheimer's disease (AD), a progressive neurodegenerative disease [3]. AD is the most common cause of dementia and will afflict 11% of the United States population over the age of 65 costing the nation \$226 billion in 2015 alone [4]. It is estimated that by 2050, the worldwide incidence of AD will triple unless innovative strategies, including dietary intervention, are implemented in addition to lifestyle changes and chronic disease management [5].

The extensive neuronal loss that leads to functional and memory impairments in AD patients has been attributed to the proteotoxicity of extracellular amyloid-beta (A $\beta$ ) plaques and intracellular tau neurofibrillary tangles [6, 7]. Several pharmacological therapies focus on interrupting the underlying pathogenesis of AD in the brain [8]. While a common target is A $\beta$  plaques, these approaches have largely been unsuccessful due to limitations in current scientific understanding of all of the etiological and pathophysiological factors relevant in AD. Therefore, there is a critical need to discover new therapeutic approaches to manage AD, especially since several drugs currently in clinical evaluation have been associated with severe side effects in patients [9]. Consequently, similar to several other chronic human diseases, the integration of natural products as part of a non-toxic dietary intervention strategy holds great promise for AD prevention [10]. This is due, in part, to the multi-mechanistic modes of action exerted by natural compounds, whereby, they could potentially prevent and/or delay the deleterious effects of oxidative stress, neuroinflammation, proteotoxicity, and other factors implicated in the pathogenesis of neurodegenerative diseases.

Published data suggest that several phenolic-rich plant foods including certain fruits, berries, spices, nuts, green tea, and olive oil may show promise for AD prevention [10]. Phenolic compounds include a chemically diverse group of secondary metabolites containing a phenolic moiety which are prevalent in plant foods and their derived products. Indeed, dietary plant extracts and their purified phenolic constituents such as resveratrol (from grape and red wine) [10], anthocyanins (from berries) [11], curcumin (from turmeric spice) [12], oleocanthal (from olive oil) [13], and catechin (from grape seed) [14], have been studied extensively for their biological effects against AD. Several studies have noted that the biological activities of these single purified molecules are potentiated by synergistic, additive, and/or complementary effects of multiple (minor) constituents present in their

respective phenolic-enriched ‘whole’ plant extracts [15]. Thus, chemically standardized botanical extracts, delivered in food, supplement, and pharmaceutical matrices, hold great promise for the prevention of neurodegenerative diseases in future human clinical studies.

Maple syrup is a plant-derived natural sweetener obtained by boiling the sap collected primarily from the sugar maple (*Acer saccharum*) species. Apart from its predominant constituent which is sucrose, maple syrup also contains oligosaccharides, amino acids, organic acids, vitamins, minerals, and phytohormones [16]. In addition, a large number of natural phenolic compounds originally present in the xylem sap of the sugar maple plant survive the boiling process and persist in maple syrup [16–19]. However, despite the wide consumption of maple syrup worldwide, and knowledge that it contains a diverse array of phenolic constituents (over fifty phenolics belonging to lignan, stilbene, flavonoid, coumarin, and phenolic acid sub-classes have been isolated and identified from maple syrup) [17–19, 22], studies evaluating their health promoting effects are very limited. Moreover, based on our knowledge to date, few studies have been conducted to evaluate the neuroprotective effects of this natural sweetener [20, 21]. In one of those studies, a phenolic-enriched maple syrup extract was shown to decrease oligomerization and aggregation of both A $\beta$ <sub>1–42</sub> and tau peptides, which are proteins involved in AD pathogenesis [20]. In light of the aforementioned factors, and given the paucity of data on the neuroprotective effects of natural plant-derived sweeteners, including maple syrup, we designed the current study.

Our group has previously reported on the chemical standardization of a food grade phenolic-enriched maple syrup extract (named MSX) for nutraceutical applications [22]. This extract contains the natural phenolic constituents, as well as other substances (amino acids, organic acids, minerals, and oligosaccharides) present in the whole maple syrup food but with reduced sucrose content. MSX is well tolerated and its safety has been established in animal studies (in Sprague-Dawley rats) [22]. Notably, MSX shows anti-inflammatory effects (based on in vitro studies in RAW264.7 macrophages) superior to any of its purified phenolic constituents alone [23]. Therefore, given the aforementioned factors about the additive and synergistic effects observed with ‘whole’ plant extracts [15], as well as the possibility of a nutraceutical/botanical supplement being utilized as a dietary intervention strategy in future human clinical studies, we have chosen to advance our studies on this natural product by evaluating MSX rather than any of its purified single constituents alone.

Herein, we sought to evaluate the neuroprotective effects of MSX against AD using a combination of biophysical (Thioflavin T assay, transmission electron microscopy, circular dichroism, dynamic light scattering, and zeta potential), in vitro (in murine BV-2 microglial, and human SY-SY5Y neuronal cells) and in vivo (in *Caenorhabditis elegans*) studies. This is the first study to evaluate the effects of maple syrup constituents on markers of oxidative and inflammatory stresses in brain cells and its potential to delay A $\beta$ <sub>1–42</sub> induced neurotoxicity and paralysis in an in vivo AD model.

## Materials and Methods

### Chemicals

Human amyloid peptide 1–42 ( $\text{A}\beta_{1-42}$ ) was purchased from AnaSpec (Fremont, CA, USA). Resveratrol (RESV), Folin-Ciocalteu reagent, thioflavin T (ThT), 2',7'-dichlorofluorescin diacetate (DCFDA), lipopolysaccharide (LPS) and solvents were purchased from Sigma-Aldrich (St. Louis, MO, USA). Uranyl acetate was purchased from Structure Probe Inc. (West Chester, PA, USA). ELISA kits for prostaglandin E2 (PGE<sub>2</sub>), and tumor necrosis factor  $\alpha$  (TNF $\alpha$ ) and interleukin-6 (IL-6) were purchased from Cayman Chemical (Ann Arbor, MI, USA), and Abcam (Cambridge, MA, USA), respectively.

### Phenolic-enriched maple syrup extract (MSX)

The phenolic-enriched maple syrup extract (MSX), was prepared according to our previously reported methods [19, 22, 23]. The details of the MSX preparation and its chemical characterization (by HPLC-DAD analyses by comparison to authentic phenolic standards previously isolated from maple syrup), the structures of the compounds identified therein, and the carbohydrate (sucrose, glucose and fructose) and phenolic (by Folin-Ciocalteu assay based on gallic acid equivalents, GAEs) contents, are provided in the Supplementary Materials.

### $\text{A}\beta_{1-42}$ thioflavin T (ThT) binding assay

$\text{A}\beta_{1-42}$  solutions were prepared following previously reported methods with minor modifications [24]. In brief, fibril formation was induced by incubating 50  $\mu\text{M}$   $\text{A}\beta_{1-42}$  solutions at 37 °C for 5 d. Treatment included MSX at varying concentrations (50, 100, 200 and 500  $\mu\text{g}/\text{mL}$ ) and the widely studied neuroprotective polyphenolic compound, resveratrol (RESV), used as the positive control (at 50  $\mu\text{g}/\text{mL}$ ). The ThT binding assay was used to evaluate  $\text{A}\beta_{1-42}$  fibrillation by adding ThT solution (200  $\mu\text{L}$ ) at a concentration of 10  $\mu\text{M}$  to each sample (50  $\mu\text{L}$ ). The intrinsic fluorescence was immediately measured using a Spectra Max M2 spectrometer (Molecular Devices, Sunnyvale, CA, USA) at excitation and emission wavelengths of 450 and 483 nm, respectively. Percent inhibition (% inhibition) of each treatment was calculated based on arbitrary fluorescence (FU) by the following equation: % inhibition = [(FU of control – FU of treatment)/FU of control] × 100%.

### Transmission electron microscope (TEM) analyses

$\text{A}\beta_{1-42}$  solutions for TEM analysis were prepared under the same conditions as the ThT binding assay.  $\text{A}\beta_{1-42}$  fibril formation was visualized by TEM as previously reported [25, 26]. The blank, control, and MSX (500  $\mu\text{g}/\text{mL}$ ) treated samples (5  $\mu\text{L}$  each) were placed onto a 200 mesh carbon-coated copper TEM grid (Ted Pella Inc., Redding, CA, USA) for 2 min. The excess fluid was removed by filter paper and 5% uranyl acetate (10  $\mu\text{L}$ ) was placed onto the grid for 2 min.  $\text{A}\beta_{1-42}$  fibril formation was imaged using a Joel Corp. (Peabody, MA, USA) JEM 2100 TEM with a LaB6 illumination filament operating at 200 kV.

### Circular dichroism (CD) analyses

The change in the secondary structure of A $\beta$  solutions were measured using a Jasco J-1100 CD spectropolarimeter (Jasco, Tokyo, Japan). Analyzed samples included 50  $\mu$ M native A $\beta$ <sub>1-42</sub> solution (non-incubated) and the aforementioned fibril-enriched A $\beta$  solutions. CD measurements were carried out in the far-ultraviolet region from 190–260 nm using a quartz cuvette with a path length of 0.1 cm. The bandwidth was set at 1 nm for each run and 5 repetitive scans were obtained. The Selcon 3 method was applied to calculate the secondary structure composition using CDPro software (Jasco, Tokyo, Japan).

### Dynamic light scattering (DLS) and zeta potential measurement

The size of A $\beta$ <sub>1-42</sub> aggregates and zeta potential were measured with a Zetasizer Nano-ZS90 (Malvern, Worcestershire, UK) as previously reported for the analyses of amyloid fibril formation [27]. Test samples included: 1) 50  $\mu$ M freshly prepared A $\beta$ <sub>1-42</sub>, 2) 50  $\mu$ M A $\beta$ <sub>1-42</sub> aggregated at 37 °C for 5 d and, 3) 50  $\mu$ M aggregated A $\beta$ <sub>1-42</sub> co-treated with MSX (500  $\mu$ g/mL) for 5 d. Each measurement represents the average of three independent experiments and 100 consecutive runs were obtained for each sample at an operating temperature of 25 °C.

### Cell culture

The BV-2 murine microglial cells were a gift from Dr. Grace Y. Sun (University of Missouri at Columbia, MO, USA) and the SH-SY5Y (human neuroblastoma) cells were obtained from the American Type Culture Collection (ATCC). Cell lines were maintained using high glucose (4.5 g/L) DMEM/F12 (Life Technologies, Gaithersburg, MD, USA) supplemented with 10% heat inactivated FBS (Life Technologies, Gaithersburg, MD, USA), 1% P/S (100 U/ml penicillin, 100  $\mu$ g/ml streptomycin) (Life Technologies, Gaithersburg, MD, USA) and incubated in 5% CO<sub>2</sub> at 37°C. After reaching a confluence of 85%, the SH-SY5Y cells were differentiated for 7 d using all-trans retinoic acid (10  $\mu$ M) while changing media every 48 h to ensure proper neurite growth and cell morphology. All samples were dissolved in DMSO (Sigma Aldrich, St. Louis, MO, USA) to yield a 10 mg/mL stock solution. Samples were further diluted to yield solutions with a final DMSO concentration of less than 0.1%.

### Measurement of cell viabilities

Cell viabilities of BV-2 and SH-SY5Y cells were evaluated using the MTT [3-(4,5-dimethylthiazol-2-yl)-2,5-diphenyltetrazolium bromide] colorimetric assay [28] and CellTiter-Glo 2.0 (CTG 2.0) one step assay (Promega Fitchburg, WI, USA), respectively. Briefly, in the MTT assay, BV-2 cells were seeded into 48-well plates at a density of 10<sup>4</sup> cells/well in DMEM. After 24 h, the cells were treated with MSX (50 or 100  $\mu$ g/mL) for 48 h. At the end of the treatment, the cell viability was measured by using cell-counting kit 8 reagent (Dojindo Molecular Technologies, Rockville, MD, USA), according to the manufacturer's instructions. In the CTG 2.0 assay, SH-SY5Y cells were seeded at 10<sup>-5</sup> cells/mL to yield 80–85% confluence in a standard white walled clear bottom 96-well plate after 24 h initial incubation. Following a secondary incubation period (24 h), CTG 2.0 was added in a 1:1 ratio with the existing media in the wells and mixed for 2 min on an orbital

shaker prior to luminescence measurement using the Spectramax M2 (Molecular Devices Sunnyvale, CA, USA).

#### **Measurement of levels of reactive oxygen species (ROS)**

BV-2 cells were seeded into 48-well plates at a density of  $10^4$  cells/well in DMEM. After 24 h, the cells were pretreated with MSX (50 or 100  $\mu$ g/mL) or the positive control, resveratrol (RESV; 5  $\mu$ g/mL) for 24 h. Then, the medium was replaced with DMEM containing 20  $\mu$ M DCFDA for 20 min. The cells were washed with phosphate buffered saline and incubated with H<sub>2</sub>O<sub>2</sub> at a non-toxic concentration (3.0  $\mu$ g/mL) for 1 h. The fluorescence signal was read at excitation and emission wavelengths of 485 and 525 nm, respectively, using a Spectra Max M2 spectrometer (Molecular Devices, Sunnyvale, CA, USA).

#### **Measurement of nitric oxide species (NOS) levels by Griess assay**

BV-2 microglial cells in 24-well plates ( $n = 4$ ) at 85% confluence ( $10^5$  cells/well) were serum-starved for 4 h prior to the treatments. Then the cells were incubated with MSX (50 or 100  $\mu$ g/mL) or the positive control, resveratrol (RESV; 5  $\mu$ g/mL) for 1 h before lipopolysaccharide (LPS) was added. After 23 h incubation, the cell culture media were collected and centrifuged. The supernatants were measured for total nitric oxide (NO) levels using the Griess assay kit (Promega, Fitchburg, WI, USA) as previously reported [23]. Sodium nitrite, at different dilutions, was used to generate a standard curve which was used to calculate nitrite concentrations.

#### **Measurements of IL-6, PGE<sub>2</sub>, and TNF $\alpha$ levels**

Supernatants collected from the NO experiments above were collected and assayed for inflammatory cytokines including interleukin-6 (IL-6), prostaglandin E2 (PGE<sub>2</sub>) and tumor necrosis factor  $\alpha$  (TNF $\alpha$ ). Quantification of PGE<sub>2</sub> and TNF $\alpha$  were measured using enzyme linked immunosorbent assay (ELISA) kits based on the respective manufacturer protocols.

#### **Non-contact co-culture model with BV-2 and SH-SY5Y cells**

BV-2 and SH-SY5Y cells were co-cultured as previously reported [29–31]. Briefly, BV-2 and differentiated SH-SY5Y cells (both cell lines at a density of  $10^5$  cells/mL) were plated in 12-well and 96-well plates, respectively, and allowed to attach for 24 h. The BV-2 cells were then exposed to MSX (50 and 100  $\mu$ g/mL) or RESV (5  $\mu$ g/mL; positive control) for 1 h prior to exposure to LPS (1  $\mu$ g/mL) for a duration of 24 h of treatment. Conditioned media were then collected from the BV-2 cells and centrifuged at 18,000 rcf for 5 min at 4°C. The media from the SH-SY5Y cells was removed and replaced with the centrifuged conditioned media from the BV-2 cells and left to incubate for 24 h after which they were subjected to the CTG 2.0 assay to assess cell viability.

#### **Transgenic *Caenorhabditis elegans* in vivo assay**

The *C. elegans* nematode assay was carried out as previously reported by our group [24]. Briefly, the transgenic *C. elegans* strain CL4176, developed to express human amyloid  $\beta_{1-42}$  in the muscle tissue in response to heat shock, were obtained from the Caenorhabditis Genetics Center (CGC) (University of Minnesota, Minneapolis, MN, USA). Worms were

Author Manuscript  
Author Manuscript  
Author Manuscript  
Author Manuscript

grown and maintained at 16 °C on 60 mm culture plates with Nematode Growth Medium (NGM). Media was poured aseptically into culture plates (10 mL for 60 mm) using a peristaltic pump and allowed to solidify for 36 h. NGM culture plates were then inoculated with 50 µL of *Escherichia coli* OP50 (CGC, University of Minnesota, Minneapolis, MN, USA) overnight cultures and incubated for 8 h at 37 °C. The *C. elegans* were maintained by picking 2–3 young adult worms onto freshly inoculated NGM plates every 4–7 d. MSX was dissolved in S-basal buffer and methanol solution (1:1; v/v) and further diluted in S-basal buffer to a yield a final concentration of 1 mg/mL which served as the stock solution. The MSX stock solution was added directly to the NGM media for a final treatment concentration of 10 µg/mL. Upon development of the eggs to the L3 larval stage, the incubation temperature of the plates was increased from 16 to 25 °C to induce the expression of Aβ<sub>1–42</sub>. Mobility scoring was conducted beginning at 20 h after the temperature increase and continued in 2 h increments until all of the worms were paralyzed. Failure to respond to touch (prodding with a worm pick) and, absence of pharyngeal pumping, were used to score paralyzed/dead worms.

### Statistical analyses

Data are presented as mean ± standard deviation of at least 3 separate experiments. For the ThT assay, statistical analysis was conducted by one-way factorial ANOVA with Tukey-Kramer post hoc comparisons. Cellular assay data were expressed as means ± standard errors. *P* values were generated using ANOVA followed by Dunnett's test for multiple comparisons of group means. For the *in vivo* *C. elegans* assay, the Kaplan-Meier method was used to compare the lifespan survival curves and the survival differences were tested for statistical significance using the Log rank test (Mantel Cox). Significance for all tests was defined as: *p* < 0.05 (\*), *p* < 0.01 (\*\*), *p* < 0.001 (\*\*\*), and *p* < 0.0001 (\*\*\*\*). GraphPad Prism software 6.0 (GraphPad Software, Inc., San Diego, CA) was used for all statistical analysis calculations.

## Results and discussion

### Chemical characterization of phenolic-enriched maple syrup extract (MSX)

MSX is a chemically standardized food grade phenolic-enriched maple syrup extract, previously developed by our group for nutraceutical applications, with established safety and tolerability data in animals [22]. For the present study, MSX was prepared in our laboratory based on methods previously reported by our group (details provided in Supplementary Materials).

Our group has previously isolated and identified (using NMR and mass spectrometry) over fifty phenolic compounds from maple syrup [19, 22, 23]. Therefore, through comparison of HPLC-DAD retention times with these chemical marker standards, as shown in Fig. 1, a total of thirty-seven compounds (chemical structures provided in Fig. S2 in the Supplementary Materials) were identified in MSX. As expected, the majority of the compounds in MSX are phenolic compounds, belonging to lignan, coumarin, phenolic acid, and stilbene sub-classes.

The phenolic content of MSX used in the present study was determined as 24.0% (based on gallic acid equivalents, GAEs). In addition, it had a sucrose content of ca. 10.0% as compared to pure maple syrup which was 63%. The levels of fructose and glucose in MSX were < 0.1%. We next sought to evaluate the neuroprotective effects of MSX using a combination of biophysical (Thioflavin T assay, transmission electron microscopy, circular dichroism, dynamic light scattering and zeta potential), *in vitro* (murine BV-2 microglial, and human SH-SY5Y cells) and *in vivo* (*Caenorhabditis elegans*) studies (further described below).

### MSX inhibits A $\beta$ fibrillation

A $\beta$  deposition in brain leads to the formation of senile plaques and causes neurotoxicity in AD patients. During the progression of AD, soluble unstructured A $\beta$  peptides gradually reassemble to insoluble A $\beta$  fibrils, a structure enriched in  $\beta$ -sheet confirmation. Therefore, MSX was evaluated for its inhibitory effects on the formation of A $\beta_{1-42}$  fibril structures using a combination of biophysical methods. A $\beta_{1-42}$  fibrillation was first quantified by the fluorescence based ThT binding assay (Fig. 2A) and the morphology of the fibrils was visualized by TEM (Fig. 2B). The  $\beta$ -sheet contents were measured by circular dichroism (CD) studies (Fig. 3). The size and zeta potential of A $\beta_{1-42}$  aggregates were measured by zetasizer (Table 1).

As shown in Fig. 2A, the control generated the highest binding level in the ThT assay indicating that the control group had the highest level of A $\beta_{1-42}$  fibrillation. The A $\beta_{1-42}$  fibrillation level significantly decreased in all of the treatment samples including the different concentrations of MSX (from 50–500  $\mu$ g/mL) and the neuroprotective polyphenolic compound, resveratrol (RESV), used as a positive control. The data generated in the current study for RESV (50  $\mu$ g/mL, inhibition = 77.3%,  $p$  0.001) is in agreement with previously published data [32]. Similarly, the MSX treated solutions showed a concentration-dependent effect at 500, 250, 100 and 50  $\mu$ g/mL, reducing A $\beta$  fibrillation by 63.5, 55.9, 54.9 and 18.9%, respectively. Therefore, the ThT assay data suggested that both MSX and RESV significantly inhibited A $\beta$  fibrillation. Also, it should be noted that the lowest test concentration of MSX (50  $\mu$ g/mL) significantly inhibited the formation of A $\beta_{1-42}$  fibrils ( $p$  0.05).

Our findings from the ThT assay were further confirmed by the TEM analyses. As shown in Fig. 2B, the control A $\beta_{1-42}$  sample generated morphology of aggregates typically seen in the fibrillation process of A $\beta_{1-42}$  [25, 26]. In contrast, the A $\beta_{1-42}$  co-treated with MSX (500  $\mu$ g/mL) sample showed a different morphology compared to the control. The overall fibrils in the MSX treated solution were significantly less dense but more amorphous, indicating that the formation of highly ordered A $\beta$  fibrils was reduced by MSX.

Next, we measured the  $\beta$ -sheet contents in A $\beta_{1-42}$  solutions using CD spectroscopy (shown in Fig. 3 and Table 1). Compared to native non-aggregated A $\beta_{1-42}$ , all of the incubated samples displayed a signature dip at 220 nm, indicating the formation of  $\beta$ -sheets structures [33]. However, in the MSX treated sample (500  $\mu$ g/mL), the conformational changes of the  $\beta$ -sheets were 10% lower than that of control (49.6 vs. 59.6%). A similar trend was observed for the positive control, RESV (50  $\mu$ g/mL), which showed a  $\beta$ -sheet content of 46.7%.

$\text{A}\beta_{1-42}$  fibrillation can cause the formation of aggregates which can be measured by dynamic light scattering (DLS) [27]. Based on DLS measurements (shown in Table 1), no measurable aggregates were observed in native freshly prepared  $\text{A}\beta_{1-42}$ . In contrast, after incubation at 37 °C,  $\text{A}\beta_{1-42}$  yielded aggregates with particle size of 317.9 nm and a dominant content of 86.4% which were reduced to 39.84 nm and 77%, respectively, by MSX (500 µg/mL). As previously reported, the zeta potential of  $\text{A}\beta_{1-42}$  shifts to a more negative value as aggregation progresses [27]. Our data is in agreement with these observations [27] wherein we observed a significant decrease in zeta potential values from -4.58 mV for freshly prepared  $\text{A}\beta_{1-42}$  to -22.4 mV for aggregated  $\text{A}\beta_{1-42}$ . However, the MSX treated  $\text{A}\beta_{1-42}$ , generated an increase in zeta potential value of -17.6 mV, indicating that the aggregation process was less extensive than the control.

Taken together, the biophysical data from the ThT assay, TEM analyses, CD experiment, DLS, and zeta potential measurements suggested that the MSX treatments effectively inhibited  $\text{A}\beta_{1-42}$  structural transformation from soluble non-toxic peptides to insoluble neuro-toxic fibrils. These data are in agreement with the previous report for a phenolic-enriched maple syrup extract [20]. However, to date, no previous studies have been conducted to evaluate the neuroprotective effects of maple syrup in brain cells or in an *in vivo* AD model; therefore, we proceeded with the following experiments (described below).

### **MSX protects murine BV-2 microglia against $\text{H}_2\text{O}_2$ -induced oxidative stresses *in vitro***

Microglia cells are resident innate immune cells in the central nervous system with a similar functional role as macrophages. An important cellular response in neurodegenerative diseases pathogenesis is microglial activation. Moreover, the over-activation of microglia can lead to the release of a variety of pro-inflammatory mediators which are potentially neurotoxic. This activation process is often promoted by cellular oxidative stress factors including reactive oxygen species (ROS) and thus, the reduction of ROS levels alleviates microglial activation and related neuronal disorders [34]. Therefore, MSX was evaluated (at non-toxic concentrations, ranging from 10 to 100 µg/mL based on the MTT assay, as shown in Fig. 4A) for its effects on  $\text{H}_2\text{O}_2$  (3.0 µg/mL) induced ROS production in murine BV-2 microglia cells. As shown in Fig. 4B, MSX decreased  $\text{H}_2\text{O}_2$ -induced ROS production in BV-2 cells. At concentrations of 50 and 100 µg/mL, MSX reduced  $\text{H}_2\text{O}_2$ -induced ROS production by 9.9 and 16.1%, respectively. The positive control, RESV, decreased  $\text{H}_2\text{O}_2$ -induced ROS levels by 66.2% at a concentration of 5 µg/mL, which was similar to previously reported data [34].

### **MSX protects murine BV-2 microglia against LPS-induced inflammatory stresses *in vitro***

Our group has previously shown that MSX reduced pro-inflammatory cytokines in RAW264.7 murine macrophages [23] but to date, these effects have not been investigated in brain cells. Herein, we evaluated whether MSX could reduce levels of biomarkers for neuronal inflammation, induced by LPS, in BV-2 cells. Indeed, the LPS treated cells produced higher NO levels compared to untreated cells (51.9 vs 9.2 µM). As shown in Fig. 5A, MSX inhibited NO production. At 50 and 100 µg/mL, MSX decreased NO production by 10.0 and 22.1%, respectively. Similar to previously reported data [34], RESV (5 µg/mL), reduced LPS-induced NO production by 23%.

Next, MSX was further evaluated for its effects on inflammatory cytokines, IL-6, PGE<sub>2</sub> and TNF $\alpha$ , in the BV-2 cells. As shown in Fig. 2A, after incubation of the BV-2 microglial cells with LPS, MSX (100  $\mu$ g/mL) significantly (by 19.9%) reduced IL-6 levels as compared to the LPS treated control cells. However, the IL-6 production was not significantly (4.2 %) reduced by treatment of MSX at the lower concentration of 50  $\mu$ g/mL. The levels of PGE<sub>2</sub> were reduced by 52.9 and 74.8%, after treatment with 50 and 100  $\mu$ g/mL MSX, respectively, compared to LPS treated control cells. In comparison, the positive control, RESV (5  $\mu$ g/mL), reduced PGE<sub>2</sub> levels by 22.5% which was similar to previously reported data [34] (Fig. 5C). Similarly, the levels of TNF $\alpha$  were down-regulated by treatment of BV-2 cells with MSX (Fig. 5D) by 75.2 and 87.6%, after treatment with 50 and 100  $\mu$ g/mL MSX, respectively, compared to the LPS treated cells. The positive control, RESV (5  $\mu$ g/mL), decreased TNF $\alpha$  levels by 31.4% similar to previously reported data [34].

### **MSX reduces cytotoxicity of human SH-SY5Y neuronal cells after exposure to murine BV-2 microglia conditioned media**

Co-culture systems have been employed to investigate the impact of microglia and its inflammatory mediators on the cell death of neurons [29–31, 35]. Therefore, we used a non-contact cell culture model (using conditioned media) to evaluate the protective effects of MSX against neurotoxicity (induced by inflammatory biomarkers released by LPS-stimulated BV-2 microglia) of differentiated human SH-SY5Y neuronal cells as previously reported [30, 31]. As shown in Fig. 6, media from BV-2 cells (treated with LPS alone) significantly decreased (15.0%) the cell viability of differentiated SH-SY5Y neuronal cells. On the contrary, the conditioned media from BV-2 cells treated with MSX (at 100 and 50  $\mu$ g/mL) reduced SH-SY5Y neuronal cell death by 17.7 and 13.8%, respectively. The positive control, RESV (5  $\mu$ g/mL), decreased the SH-SY5Y neuronal cell death by 30.5%. This observation indicated that MSX was able to ameliorate microglia-mediated neuronal cell death possibly by decreasing the production of inflammatory biomarkers by the microglia.

### **MSX protects A $\beta$ <sub>1–42</sub> induced neurotoxicity and paralysis in *Caenorhabditis elegans* in vivo**

We next evaluated the effects of MSX in an established *C. elegans* in vivo model of AD [24]. The mobility curves for the *C. elegans* CL4176 strain after the A $\beta$ <sub>1–42</sub> induction of muscular paralysis at 25 °C are shown in Fig. 6. Compared to the control worms (Fig. 7A), treatment with 10  $\mu$ g/mL MSX did not have any significant effect on the median survival/mobility in *C. elegans* post induction of A $\beta$ <sub>1–42</sub> induced neurotoxicity and paralysis. However, MSX treatment (Fig. 7B) significantly increased the maximum survival/mobility by 3.0% and decreased the mean survival/mobility post induction of A $\beta$ <sub>1–42</sub> induced neurotoxicity and paralysis by 10.4% (as shown in Table 2).

Mitochondrial dysfunction, inflammation, oxidative stress, and activation of apoptotic signaling due to intra- and extracellular accumulation of misfolded or damaged proteins has been linked to the etiopathology of neurodegenerative diseases, including AD [36, 37]. Therefore, therapies that specifically target mediators of proteotoxicity and inflammation may be more successful in ameliorating neurodegenerative processes [38]. The transgenic AD model of *C. elegans* used in our study specifically measures the intracellular aggregation of the A $\beta$ <sub>1–42</sub> peptide in muscle tissues and permits investigation of inflammatory and

Author Manuscript  
Author Manuscript  
Author Manuscript  
Author Manuscript

proteotoxicity contributors of A $\beta$ <sub>1–42</sub> peptide aggregation and subsequent neuromuscular paralysis [24, 39, 40]. In response to treatment with MSX, the heat-shock induced aggregation of A $\beta$ <sub>1–42</sub> peptide and resultant paralysis was significantly delayed in the *C. elegans* model. These results corroborated our observations from the biophysical and in vitro studies wherein MSX reduced A $\beta$ <sub>1–42</sub> fibrillation, oxidative stress, and inflammatory cytokines. It is possible that the reduced proteotoxicity in *C. elegans* in response to MSX could be due to the presence of certain bioactive compounds that interacts with amyloidogenic proteins to prevent their oligomerization (and thus aggregation) [41]. However further studies would be required to confirm this. Overall, the current study with MSX support studies done with other natural products including coffee bean extract [42], *Ginkgo biloba* [41], curcumin, and several tropical fruit extracts [39, 40], suggesting similar mechanism/s for reducing A $\beta$ <sub>1–42</sub> aggregation by abrogating proteotoxicity and inflammation.

## Conclusion

In summary, using a combination of biophysical, in vitro, and in vivo studies, a phenolic-enriched extract of maple syrup (MSX) was shown to reduce A $\beta$ <sub>1–42</sub> fibrillation and decrease oxidative and inflammatory stresses in murine BV-2 microglial cells and SHSY-5Y neuronal cells. Furthermore, MSX imparted protective effects on A $\beta$ <sub>1–42</sub> aggregation induced neurotoxicity and paralysis in *C. elegans*. However, further in vivo studies to confirm the neuroprotective effects of MSX, and to predict a human equivalent consumption dose, are necessary given that the current data does not account for important physiological considerations such as bioavailability and metabolism. Nevertheless, these findings add to recently published data supporting the potential neuroprotective effects of maple syrup [20, 21], warranting further studies on this natural plant-derived sweetener.

## Supplementary Material

Refer to Web version on PubMed Central for supplementary material.

## Acknowledgments

The spectroscopic data were acquired from instruments located in the RI-INBRE core facility supported by Grant # P20GM103430 from the National Institute of General Medical Sciences of the National Institutes of Health. We thank Dr. Grace Y. Sun (University of Missouri at Columbia, MO, USA) for kindly providing the BV-2 murine microglial cells and Dr. Richard Kingsley and the URI TEM facility (URI Chemical Engineering) for assisting with TEM sample imaging.

## Abbreviations

<b>AD</b>	Alzheimer's disease
<b>A<math>\beta</math></b>	amyloid-beta
<b>MSX</b>	phenolic-enriched maple syrup extract
<b>ThT</b>	Thioflavin T
<b>TEM</b>	transmission electron microscopy

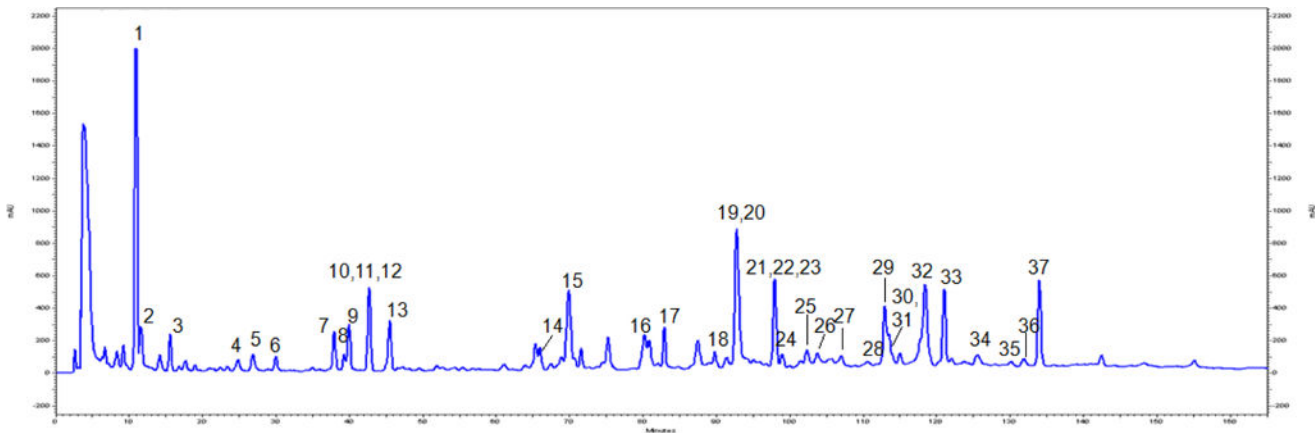
<b>CD</b>	circular dichroism
<b>DLS</b>	dynamic light scattering
<b>A<math>\beta</math><sub>1-42</sub></b>	amyloid peptide 1–42
<b>DCFDA</b>	2',7'-dichlorofluorescin diacetate
<b>LPS</b>	lipopolysaccharide
<b>RESV</b>	resveratrol
<b>DMEM/F12</b>	Dulbecco's modified eagle medium: nutrient mixture F-12
<b>FBS</b>	fetal bovine serum
<b>DMSO</b>	dimethyl sulfoxide
<b>MTT</b>	[3-(4,5-dimethylthiazol-2-yl)-2,5-diphenyltetrazolium bromide]
<b>CTG</b>	CellTiter-Glo
<b>ROS</b>	reactive oxygen species
<b>NOS</b>	nitric oxide species
<b>NO</b>	nitric oxide
<b>IL-6</b>	interleukin-6
<b>PGE<sub>2</sub></b>	prostaglandin E2
<b>TNF<math>\alpha</math></b>	tumor necrosis factor $\alpha$
<b>ELISA</b>	enzyme linked immunosorbent assay
<b>HPLC-DAD</b>	high performance liquid chromatography-diode array detection
<b>GAEs</b>	gallic acid equivalents

## References

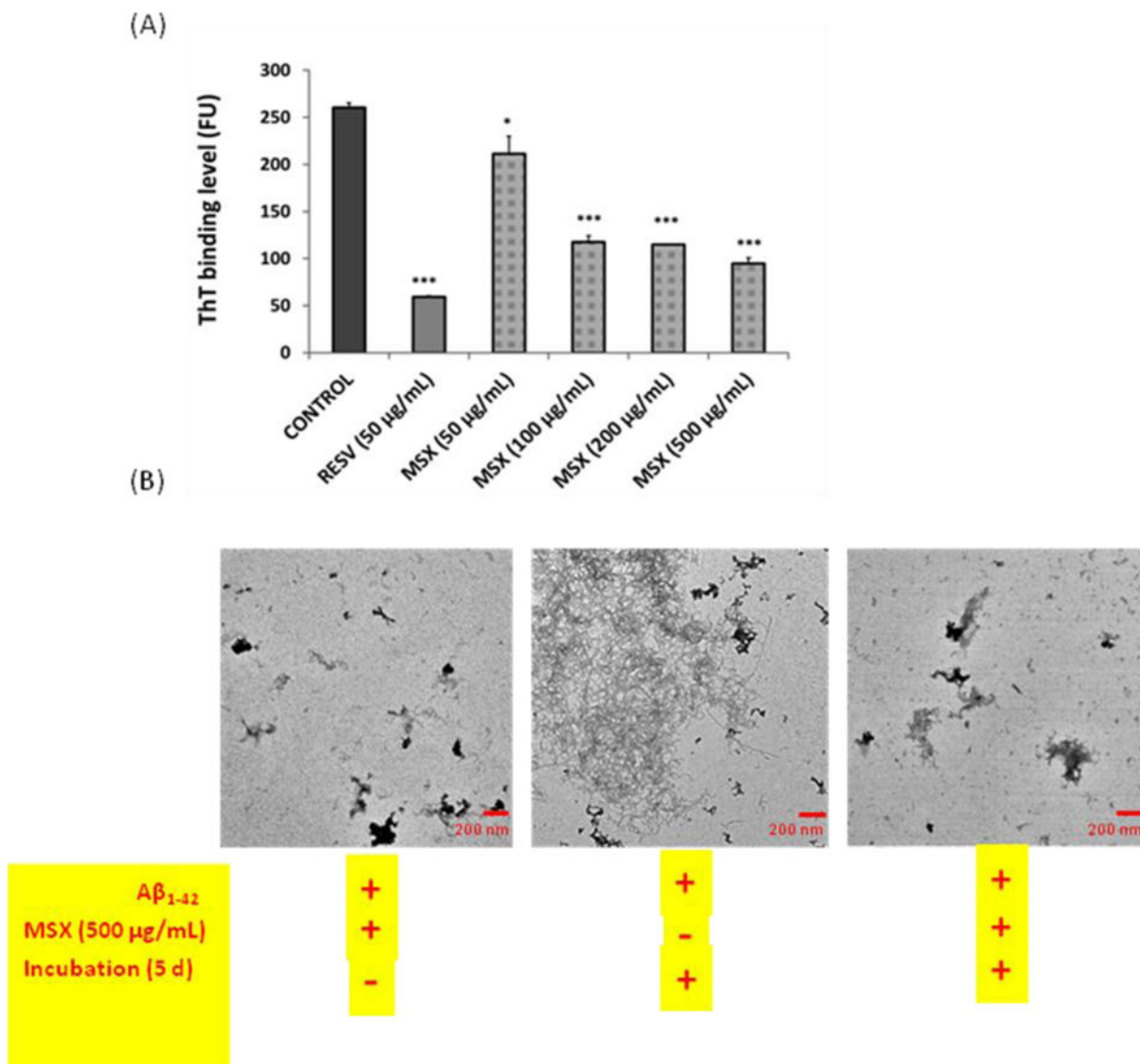
- Praticò D, Trojanowski JQ. Inflammatory hypotheses: novel mechanisms of Alzheimer's neurodegeneration and new therapeutic targets? *Neurobiol Aging*. 2000; 21:451–453. [PubMed: 10858594]
- Block ML, Zecca L, Hong J-S. Microglia-mediated neurotoxicity: uncovering the molecular mechanisms. *Nat Rev Neurosci*. 2007; 8:57–69. [PubMed: 17180163]
- Heneka MT, O'Banion MK. Inflammatory processes in Alzheimer's disease. *J Neuroimmunol*. 2007; 184:69–91. [PubMed: 17222916]
- Alzheimer's Association. 2013 Alzheimer's disease facts and figures. *Alzheimer's & Dementia*. 2013; 9:208–245.
- Sloane PD, Zimmerman S, Suchindran C, Reed P, Wang L, Boustani M, Sudha S. The public health impact of Alzheimer's disease, 2000–2050: potential implication of treatment advances. *Annu Rev Public Health*. 2002; 23:213–231. [PubMed: 11910061]
- Hardy JA, Higgins GA. Alzheimer's disease: the amyloid cascade hypothesis. *Science*. 1992; 256:184–185. [PubMed: 1566067]

7. Haass C, Selkoe DJ. Cellular processing of  $\beta$ -amyloid precursor protein and the genesis of amyloid  $\beta$ -peptide. *Cell*. 1993; 75:1039–1042. [PubMed: 8261505]
8. Herrmann N, Chau SA, Kircanski I, Lanctôt KL. Current and emerging drug treatment options for Alzheimer's disease. *Drugs*. 2011; 71:2031–2065. [PubMed: 21985169]
9. Vellas B, Pesce A, Robert PH, Aisen PS, Ancoli-Israel S, Andrieu S, Cedarbaum J, Dubois B, Siemers E, Spire J-P. AMPA workshop on challenges faced by investigators conducting Alzheimer's disease clinical trials. *Alzheimer's & Dementia*. 2011; 7:e109–e117.
10. Kim J, Lee HJ, Lee KW. Naturally occurring phytochemicals for the prevention of Alzheimer's disease. *J Neurochem*. 2010; 112:1415–1430. [PubMed: 20050972]
11. Willis LM, Shukitt-Hale B, Joseph JA. Recent advances in berry supplementation and age-related cognitive decline. *Curr Opin Clin Nutr Metab Care*. 2009; 12:91–94. [PubMed: 19057194]
12. Ringman JM, Frautschy SA, Cole GM, Masterman DL, Cummings JL. A potential role of the curry spice curcumin in Alzheimer's disease. *Curr Alzheimer Res*. 2005; 2:131–136. [PubMed: 15974909]
13. Abuznait AH, Qosa H, Busnena BA, El Sayed KA, Kaddoumi A. Olive-oil-derived oleocanthal enhances  $\beta$ -amyloid clearance as a potential neuroprotective mechanism against Alzheimer's disease: In vitro and in vivo studies. *ACS Cheml Neurosci*. 2013; 4:973–982.
14. Wang J, Ho L, Zhao W, Ono K, Rosensweig C, Chen L, Humala N, Teplow DB, Pasinetti GM. Grape-derived polyphenolics prevent A $\beta$  oligomerization and attenuate cognitive deterioration in a mouse model of Alzheimer's disease. *J Neurosci*. 2008; 28:6388–6392. [PubMed: 18562609]
15. Liu RH. Dietary bioactive compounds and their health implications. *J Food Sci*. 2013; 78(Suppl 1):A18–25. [PubMed: 23789932]
16. Ball DW. The chemical composition of maple syrup. *J Chem Edu*. 2007; 84:1647–1650.
17. Abou-Zaid MM, Nozzolillo C, Tonon A, Coppens M, Lombardo DA. High-performance liquid chromatography characterization and identification of antioxidant polyphenols in maple syrup. *Pharm Biol*. 2008; 46:117–125.
18. Li L, Seeram NP. Maple syrup phytochemicals include lignans, coumarins, a stilbene, and other previously unreported antioxidant phenolic compounds. *J Agric Food Chem*. 2010; 58:11673–11679. [PubMed: 21033720]
19. Li L, Seeram NP. Further investigation into maple syrup yields 3 new lignans, a new phenylpropanoid, and 26 other phytochemicals. *J Agric Food Chem*. 2011; 59:7708–7716. [PubMed: 21675726]
20. Hawco CL, Wang Y, Taylor M, Weaver DF. A Maple Syrup extract prevents  $\beta$ -amyloid aggregation. *Can J Neurol Sci*. 2015;1–4. [PubMed: 27482559]
21. Aaron C, Beaudry G, Parker JA, Therrien M. Maple syrup decreases TDP-43 proteotoxicity in a *Caenorhabditis elegans* model of amyotrophic lateral sclerosis (ALS). *J Agric Food Chem*. 2016; 64:3338–3344. [PubMed: 27071850]
22. Zhang Y, Yuan T, Li L, Nahar P, Slitt A, Seeram NP. Chemical compositional, biological, and safety studies of a novel maple syrup derived extract for nutraceutical applications. *J Agric Food Chem*. 2014; 62:6687–6698. [PubMed: 24983789]
23. Nahar PP, Driscoll MV, Li L, Slitt AL, Seeram NP. Phenolic mediated anti-inflammatory properties of a maple syrup extract in RAW 264.7 murine macrophages. *J Funct Foods*. 2014; 6:126–136.
24. Yuan T, Ma H, Liu W, Niesen DB, Shah N, Crews R, Rose KN, Vattem DA, Seeram NP. Pomegranate's neuroprotective effects against Alzheimer's disease are mediated by urolithins, iIIts ellagitannin-gut microbial derived metabolites. *ACS Chem Neurosci*. 2016; 7:26–33. [PubMed: 26559394]
25. Das S, Stark L, Musgrave IF, Pukala T, Smid SD. Bioactive polyphenol interactions with  $\beta$  amyloid: a comparison of binding modelling, effects on fibril and aggregate formation and neuroprotective capacity. *Food Funct*. 2016; 7:1138–1146. [PubMed: 26815043]
26. Shoval H, Weiner L, Gazit E, Levy M, Pinchuk I, Lichtenberg D. Polyphenol-induced dissociation of various amyloid fibrils results in a methionine-independent formation of ROS. *Biochim Biophys Acta*. 2008; 1784:1570–1577. [PubMed: 18778797]

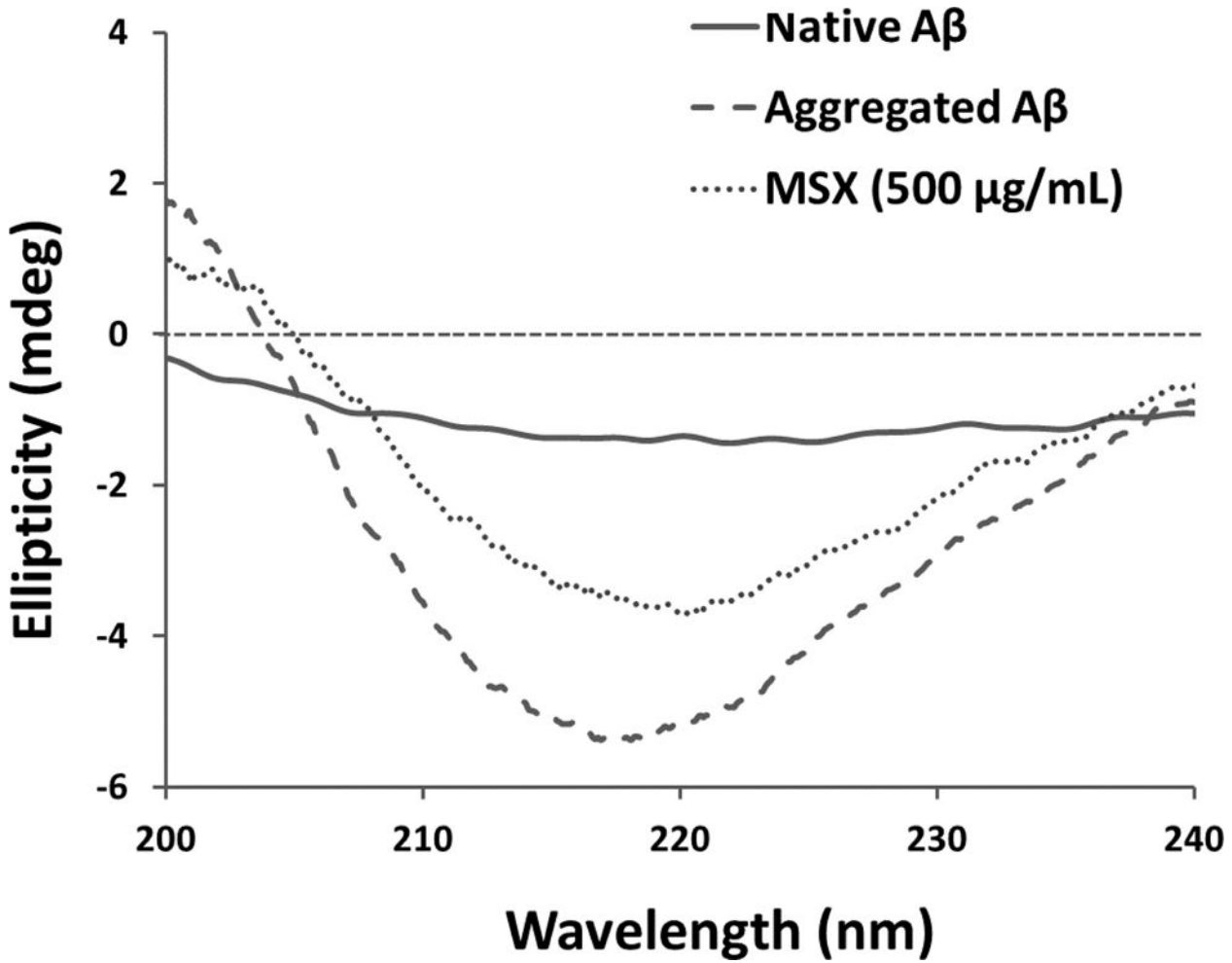
27. Vetri V, Canale C, Relini A, Librizzi F, Militello V, Gliozi A, Leone M. Amyloid fibrils formation and amorphous aggregation in concanavalin A. *Biophys Chem*. 2007; 125:184–190. [PubMed: 16934387]
28. Song X, Wei Z, Shaikh ZA. Requirement of ER $\alpha$  and basal activities of EGFR and Src kinase in Cd-induced activation of MAPK/ERK pathway in human breast cancer MCF-7 cells. *Toxicol Appl Pharmacol*. 2015; 287:26–34. [PubMed: 26006730]
29. Dowling P, Clynes M. Conditioned media from cell lines: a complementary model to clinical specimens for the discovery of disease-specific biomarkers. *Proteomics*. 2011; 11:794–804. [PubMed: 21229588]
30. Wang S, Wang H, Guo H, Kang L, Gao X, Hu L. Neuroprotection of Scutellarin is mediated by inhibition of microglial inflammatory activation. *Neuroscience*. 2011; 185:150–160. [PubMed: 21524691]
31. Liu R-P, Zou M, Wang J-Y, Zhu J-J, Lai J-M, Zhou L-L, Chen S-F, Zhang X, Zhu J-H. Paroxetine ameliorates lipopolysaccharide-induced microglia activation via differential regulation of MAPK signaling. *J Neuroinflammation*. 2014; 11:47. [PubMed: 24618100]
32. Feng Y, Wang X-P, Yang S-G, Wang Y-J, Zhang X, Du X-T, Sun X-X, Zhao M, Huang L, Liu R-T. Resveratrol inhibits beta-amyloid oligomeric cytotoxicity but does not prevent oligomer formation. *Neurotoxicology*. 2009; 30:986–995. [PubMed: 19744518]
33. Dai X, Hou W, Sun Y, Gao Z, Zhu S, Jiang Z. Chitosan oligosaccharides inhibit/disaggregate fibrils and attenuate amyloid  $\beta$ -mediated neurotoxicity. *Int J Mol Sci*. 2015; 16:10526–10536. [PubMed: 26006224]
34. Zhong L-M, Zong Y, Sun L, Guo J-Z, Zhang W, He Y, Song R, Wang W-M, Xiao C-J, Lu D. Resveratrol inhibits inflammatory responses via the mammalian target of rapamycin signaling pathway in cultured LPS-stimulated microglial cells. *PLoS one*. 2012; 7:e32195. [PubMed: 22363816]
35. Shih Y-T, Chen I-J, Wu Y-C, Lo Y-C. San-Huang-Xie-Xin-Tang protects against activated microglia- and 6-OHDA-induced toxicity in neuronal SH-SY5Y cells. *Evid Based Complement Alternat Med*. 2011; 2011:429384. [PubMed: 19339484]
36. Cohen E, Dillin A. The insulin paradox: aging, proteotoxicity and neurodegeneration. *Nat Rev Neurosci*. 2008; 9:759–767. [PubMed: 18769445]
37. Radak Z, Zhao Z, Goto S, Koltai E. Age-associated neurodegeneration and oxidative damage to lipids, proteins and DNA. *Mol Aspects Med*. 2011; 32:305–315. [PubMed: 22020115]
38. Shukla V, Mishra SK, Pant HC. Oxidative stress in neurodegeneration. *Adv Pharmacol Sci*. 2011; 1043:545–552.
39. de Fátima Bezerra M, Jamison BY, Gomada Y, Borges KC, Correia RTP, Vattem DA. *Eugenia jambolana* Lam. Increases lifespan and ameliorates experimentally induced neurodegeneration in *C. elegans*. *Int J Appl Res Nat Prod*. 2014; 7:39–48.
40. Azevêdo JC, Borges KC, Genovese MI, Correia RT, Vattem DA. Neuroprotective effects of dried camu-camu (*Myrciaria dubia* HBK McVaugh) residue in *C. elegans*. *Food Res Int*. 2015; 73:135–141.
41. Wu Y, Wu Z, Butko P, Christen Y, Lambert MP, Klein WL, Link CD, Luo Y. Amyloid- $\beta$ -induced pathological behaviors are suppressed by *Ginkgo biloba* extract EGb 761 and ginkgolides in transgenic *Caenorhabditis elegans*. *J Neurosci*. 2006; 26:13102–13113. [PubMed: 17167099]
42. Dostal V, Roberts CM, Link CD. Genetic mechanisms of coffee extract protection in a *Caenorhabditis elegans* model of  $\beta$ -amyloid peptide toxicity. *Genetics*. 2010; 186:857–866. [PubMed: 20805557]

**Fig. 1.**

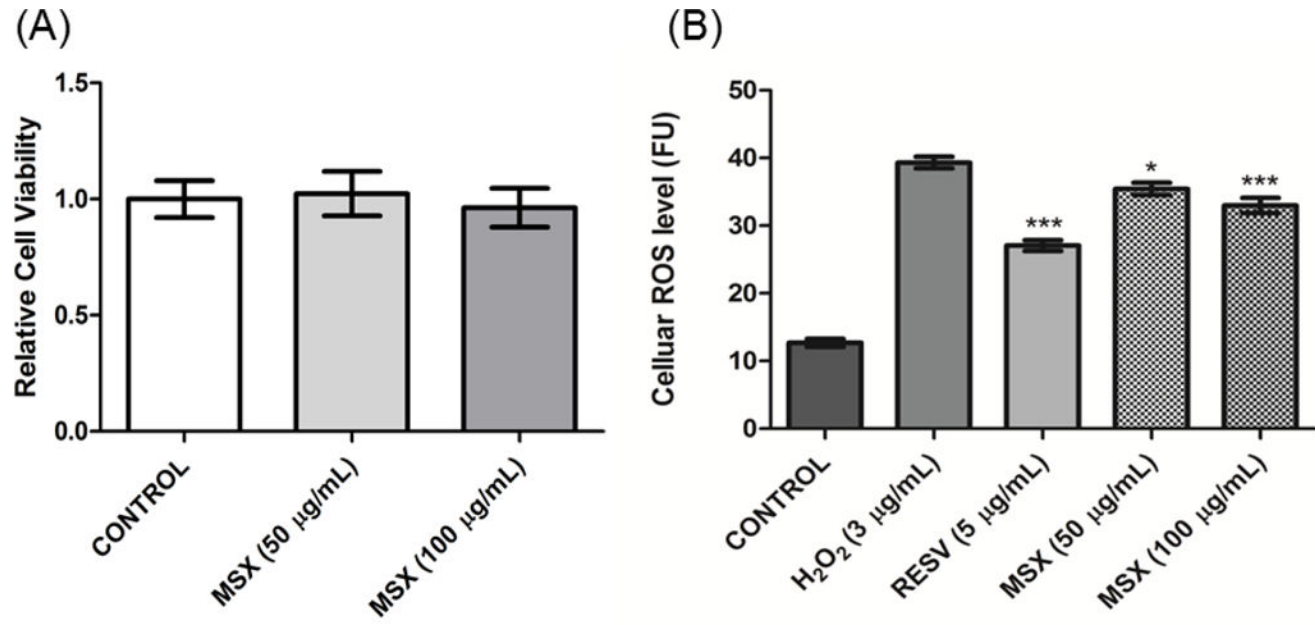
HPLC-DAD chromatogram of a phenolic-enriched maple syrup extract (MSX) showing 37 compounds identified as follows: (1) 4-hydroxy-2-(hydroxymethyl)-5-methyl-3(2*H*)-furanone, (2) 3,4-dihydro-5-(hydroxymethyl)pyran-2-one, (3) 5-(hydroxymethyl)furfural, (4) 2-hydroxy-3,4-dihydroxyacetophenone, (5) 4-(hydroxymethyl)-1,2-benzenediol, (6) catechol, (7) *C*-veratroylglycol, (8) *threo,threo*-1-[4-(2-hydroxy-2-(4-hydroxy-3-methoxyphenyl)-1-(hydroxymethyl)ethoxy)-3-methoxyphenyl]-1,2,3-propanetriol, (9) 2,3-dihydroxy-1-(4-hydroxy-3,5-dimethoxyphenyl)-1-propanone, (10) 4-acetylcatechol, (11) tyrosol, (12) catechaldehyde, (13) 1,2-diguaiaacyl-1,3-propanediol, (14) 3',5'-dimethoxy-4'-hydroxy-2-hydroxyacetophenone, (15) leptolepisol D, (16) 3,4-dihydroxy-2-methylbenzaldehyde, (17) vanillin, (18) fraxetin, (19) syringaldehyde, (20) syringenin, (21) scopoletin, (22) *threo*-guaiacylglycerol- $\beta$ -O-4'-dihydroconiferyl alcohol, (23) *erythro*-guaiacylglycerol- $\beta$ -O-4'-dihydroconiferyl alcohol, (24) 5-(3'',4''-dimethoxyphenyl)-3-hydroxy-3-(4'-hydroxy-3'-methoxybenzyl)-4-(hydroxymethyl) dihydrofuran-2-one, (25) 1-(2,3,4-trihydroxy-5-methylphenyl)ethanone, (26) *erythro*-1-(4-hydroxy-3-methoxyphenyl)-2-[4-(3-hydroxypropyl)-2,6-dimethoxyphenoxy]-1,3-propanediol, (27) icariside E4, (28) 3',4',5'-trihydroxyacetophenone, (29) dehydroconiferyl alcohol, (30) sakuraresinol, (31) secoisolariciresinol, (32) acernikol, (33) (1*S*,2*R*)-2-[2,6-dimethoxy-4-[(1*S*,3*a**R*,4*S*,6*a**R*)-tetrahydro-4-(4-hydroxy-3,5-dimethoxyphenyl)-1*H*,3*H*-furo[3,4-c]furan-1-yl]phenoxy]-1-(4-hydroxy-3-methoxyphenyl)-1,3-propanediol, (34) 2-[4-[2,3-dihydro-3-(hydroxymethyl)-5-(3-hydroxypropyl)-7-methoxy-2-benzofuranyl]-2,6-dimethoxyphenoxy]-1-(4-hydroxy-3-methoxyphenyl)-1,3-propanediol, (35) 4,4'-dihydroxy-3,3',5,5'-tetramethoxystilbene, (36) 4,4'-dihydroxy-3,3',5'-trimethoxystilbene, and (37) (*E*)-3,3'-dimethoxy-4,4'-dihydroxystilbene.

**Fig. 2.**

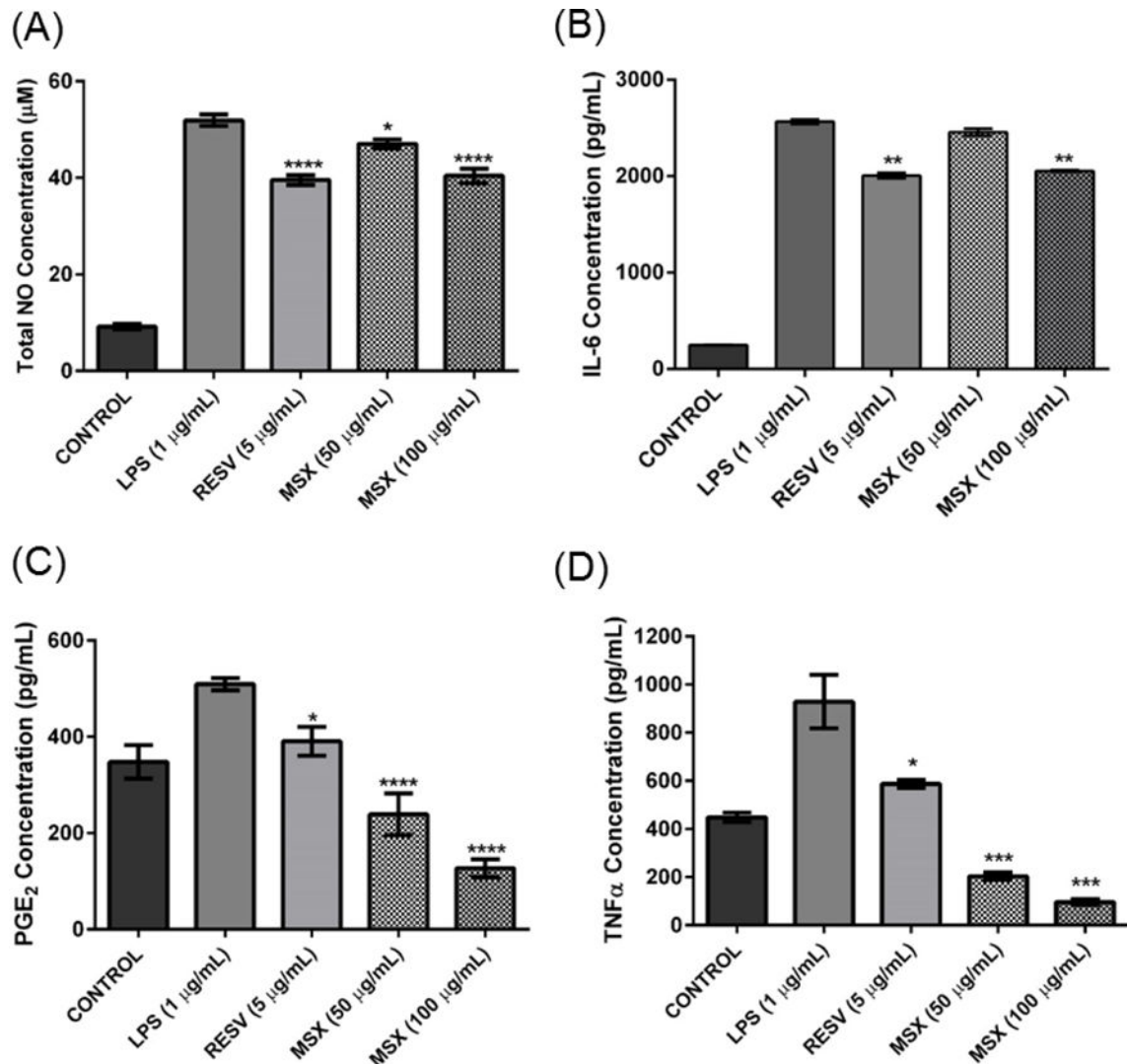
(A) ThT binding assay showing the levels of A $\beta$ <sub>1-42</sub> aggregation treated with different concentrations of MSX (50–500 µg/mL) or positive control resveratrol (RESV; at 50 µg/mL); (B) TEM analyses of A $\beta$ <sub>1-42</sub> solution freshly mixed with 500 µg/mL MSX without incubation (left), A $\beta$ <sub>1-42</sub> solution incubated for 5 d (middle) and A $\beta$ <sub>1-42</sub> solution co-treated with 500 µg/mL MSX then incubated for 5 d (right).



**Fig. 3.**  
Circular dichroism (CD) measurement of native A $\beta$ , aggregated A $\beta$ , and A $\beta$  co-treated with MSX (500  $\mu$ g/mL).



**Fig. 4.**  
MSX reduced H<sub>2</sub>O<sub>2</sub>-induced oxidative stress in BV-2 murine microglial cells. (B) BV-2 cells were pretreated with MSX (50 or 100 µg/mL) for 24 h followed by 1 h of H<sub>2</sub>O<sub>2</sub> (3 µg/mL) treatment. The H<sub>2</sub>O<sub>2</sub>-induced ROS production was measured by using the DCFDA reagent.

**Fig. 5.**

BV-2 cells pretreated with MSX (50 or 100  $\mu\text{g/mL}$ ) for 1 h followed by exposure to LPS (1  $\mu\text{g/mL}$ ) for 24 h. The treated cell culture media were used to assay the amount of NOS (A), IL-6 (B), PGE<sub>2</sub> (C), and TNF $\alpha$  (D) production. Resveratrol (RESV, at 5  $\mu\text{g/mL}$ ) served as the positive control for all the assays. Data are presented as means  $\pm$  SDs of three independent experiments.

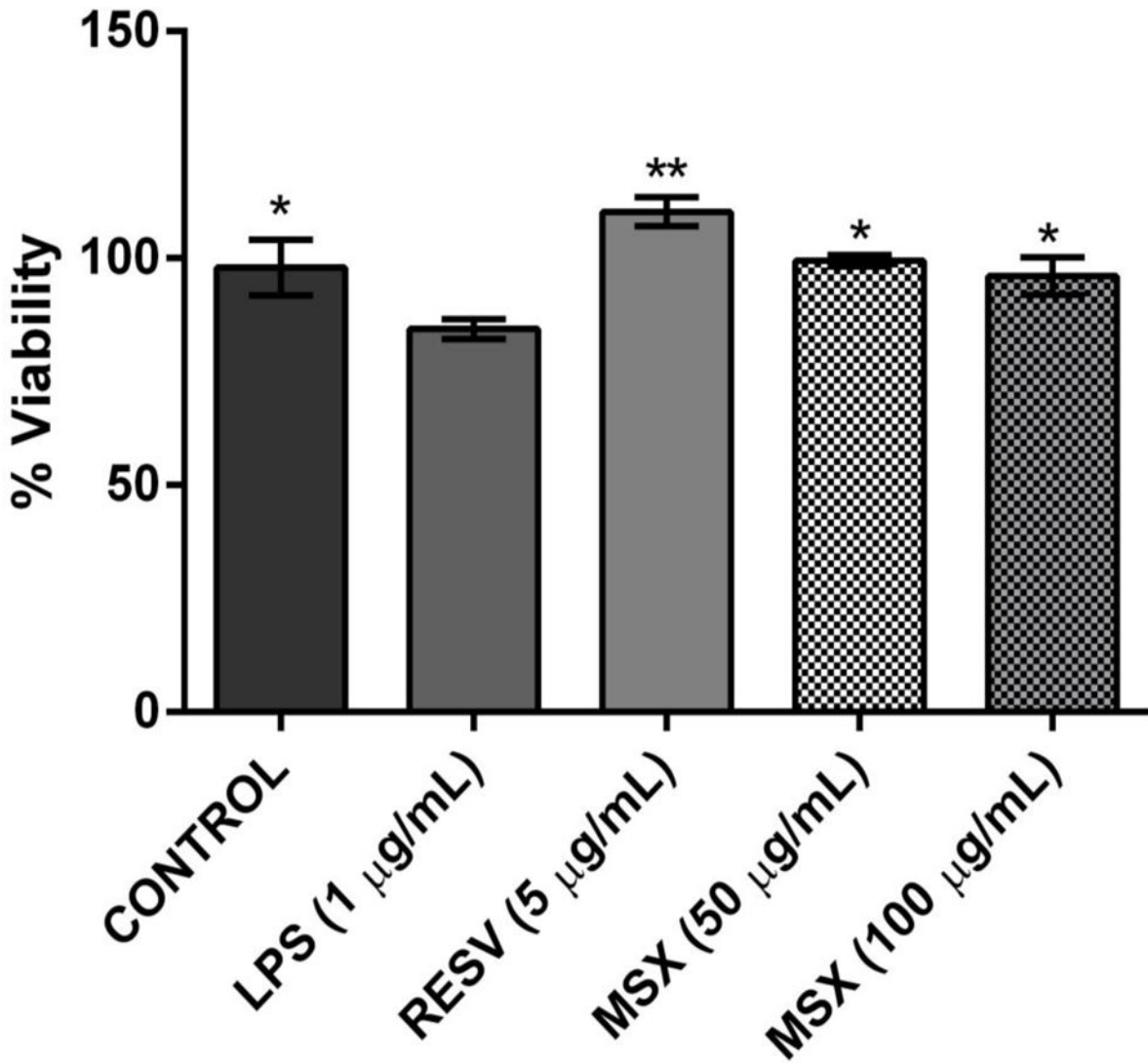


**Fig. 6.**

MSX reduced murine BV-2 microglia-mediated neurotoxicity of human SH-SY5Y neuron cells. BV-2 cells were treated with MSX (50 and 100  $\mu\text{g}/\text{mL}$ ) or resveratrol (RESV, 5  $\mu\text{g}/\text{mL}$ ; positive control) for 1 h prior to exposure to LPS (1  $\mu\text{g}/\text{mL}$ ) for 24 h. The conditioned media from the BV-2 were collected and added to SH-SY5Y cells. After incubation for 24 h, cell viability of SH-SY5Y cells were measured by the CTG 2.0 assay. All data points were compared to the LPS column.

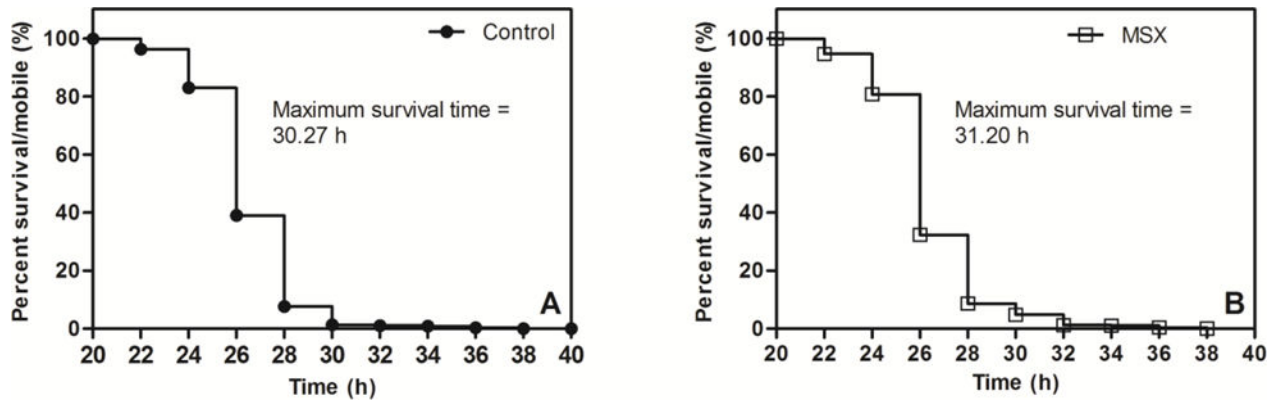


**Fig. 7.**

Mobility curves of transgenic (CL4176) *C. elegans* 20 h post A $\beta$ <sub>1-42</sub> induction of muscular paralysis at 25 °C. Kaplan-Meier mobility plots of *C. elegans* worms fed on (A) Control (NGM); (B) MSX: (NGM + 10 µg/mL MSX).

**Table 1**

Measurement of zeta potential, particle size distribution, and  $\beta$ -sheet content of native A $\beta$ <sub>1–42</sub>, aggregated A $\beta$ <sub>1–42</sub> and MSX (500  $\mu$ g/mL) treated A $\beta$ <sub>1–42</sub>. (n.d. = not detected)

	Native A $\beta$ <sub>1–42</sub>	Aggregated A $\beta$ <sub>1–42</sub>	MSX (500 $\mu$ g/mL)
Zeta Potential (mV)	−4.58	−22.4	−17.6
Particle Size (d.nm)	n.d.	317.9 (86.4%) 3.088 (13.6%)	39.84 (77.0%) 4.838 (23.0%)
$\beta$ -sheet content (%)	18.8	59.6	49.6

**Table 2**

Survival (mean, median, and maximum) of (CL4176) *C. elegans* worms treated with MSX (10 µg/mL) post Aβ<sub>1–42</sub> induction of muscular paralysis at 25 °C.

Treatment (10 µg/mL)	Survival time (h)		
	Mean	Median	Maximum
Control (n>1000)	29.60	26.00	30.27
MSX (n>1000)	26.50 *	26.00	31.20 *

\* p< 0.05; Log rank test (Mantel Cox).